

# Ultraviolet-Induced Aging of Flexographic Printing Plates Studied by Thermal and Structural Analysis Methods

C. Andersson, J. Johnson, L. Järnström

Department of Chemical Engineering, Karlstad University, SE-651 88 Karlstad, Sweden

Received 28 May 2008; accepted 25 October 2008

DOI 10.1002/app.29525

Published online 9 February 2009 in Wiley InterScience (www.interscience.wiley.com).

**ABSTRACT:** The properties of photopolymer printing plates subjected to artificial aging processes were investigated with differential scanning calorimetry and microscopic analysis. The results showed that exposure to extended ultraviolet radiation type C in the prepress process caused changes both in the thermal properties and in the structure of the outermost surface layer. Long exposure to ultraviolet radiation type A in a weathering tester led to structural changes at a deeper level and a simultaneous increase in the glass-transition temperatures of the poly-

meric material. Spectroscopic analysis showed that extensive oxidation occurred in the outermost surface layer. This study provides insight into important aging processes of the photopolymer printing plates. The knowledge can be used to predict the lifetime of printing plates and to understand the effects of their aging on print quality. © 2009 Wiley Periodicals, Inc. *J Appl Polym Sci* 112: 1636–1646, 2009

**Key words:** degradation; differential scanning calorimetry (DSC); elastomers; irradiation; photopolymerization

## INTRODUCTION

Solid-sheet photopolymer printing plates have found extensive use in the flexographic printing industry in recent years.<sup>1,2</sup> A typical solid-sheet photopolymer plate includes a thermoplastic, elastomeric multi-block copolymer based on styrene and a diene and ethylenic unsaturated acrylate compounds capable of undergoing photopolymerization to form a cross-linked network together with photoinitiators that can be activated by exposure to light.<sup>3</sup> Through control of the composition and relative proportions of the components, it is possible to create plates with a wide range of properties to meet industrial demands such as short-run printing series, high quality, and cost competitiveness and environmental concerns.<sup>4</sup>

Good performance of the printing plate is important for establishing proper contact between the anilox roll, ink, and plate and the plate, ink, and substrate in the flexographic printing process. Adequate contact is essential for a satisfactory printing result. The flexible, resilient printing plate enables flexographic printing to be applied on a wide variety of substrates, including materials with irregular surfaces.<sup>5</sup> Under normal use, the printing plate

is subjected to compression and frictional forces in the printing machine (the anilox roll and printing cylinder and the printing cylinder and substrate) that may lead to deterioration in the polymer surface.<sup>5</sup> The abrasion resistance is lower for glassy polymers, whereas rubberlike materials are more resistant to deformation and return to their original shape after being subjected to stretching, twisting, or compression.<sup>6</sup> However, repeated exposure to deformation forces will lead to a slow deterioration of the polymer properties.

The polymer plate is also subjected to the action of ink chemicals and cleaning detergents. Inappropriate ink or cleaning solvents can cause the photopolymer to either swell or shrink with subsequent cracking.<sup>7</sup> Pigment particles can cause abrasion of the polymer plate.<sup>6</sup> Storage conditions and normal aging of the polymer will also affect the lifetime of the plate.

Rubber materials are subjected to normal aging reactions that will lead to irreversible changes in the polymer properties. Sunlight, heat, oxygen, stress, atmospheric ozone, and moisture are factors that affect aging.<sup>8</sup> Free radicals can initiate oxidative degradation within the polymer, a process that is catalyzed in the presence of ultraviolet (UV) radiation and heat. The reaction of atmospheric ozone with an unsaturated elastomer can lead to the formation of ozonides and can initiate cracks in the polymer. Induced stress then leads to crack propagation, resulting in chain cleavage and the formation of decomposition products.<sup>9</sup> Ozone damage to printing plates resulting in fractures or cracks on the plate

Correspondence to: C. Andersson (caisa.andersson@kau.se).

Contract grant sponsors: Swedish Pulp and Paper Research Foundation, Knowledge Foundation, Swedish Agency for Innovation Systems, T2F Programme.

TABLE I  
Prepress Process for Digital Flexographic Printing Plates

Prepress treatment	UV radiation		Exposure time	Radiative energy (MJ/m <sup>2</sup> )	
	Type	$\lambda$ (nm)		UVA	UVC
Pre-exposure of plate back	UVA	365	50 s	0.06	0
Main exposure	UVA	365	10 min	0.73	0
Washout	—	—	20 min	—	—
Drying at 60°C	—	—	2 h	—	—
Postexposure	UVA	365	6 min	0.34	0
Light finishing	UVC	254	8 min 45 s	0	0.49
Total				1.14	0.49

surface can occur if the plate is stored close to an electric motor, in direct light, or at a high temperature.<sup>10,11</sup> Factors affecting the performance and lifetime of flexible photopolymer printing plates before their use in the printing process include shipping, unpacking, cutting, and the prepress process, during which bending and scratching of the sensitive photopolymer surface should be avoided.<sup>11</sup>

Polymer degradation can lead to discoloration, embrittlement, and deterioration of the physical properties. The basic mechanism is the absorption of light by chromophores present in the polymer, such as double bonds, or residual monomers, catalysts, aromatic or double-bond-containing contaminants, and hydroxide or carbonyl groups resulting from thermal oxidation during processing.<sup>8</sup> Vinyl polymers, including styrene, diene, and many acrylates, are particularly sensitive to UV degradation because of the presence of numerous double bonds. The same is true of styrene-isoprene-styrene (SIS) copolymers. The breakdown of chemical bonds by the action of UV energy leads to polymer fragments with a lower molecular weight and properties that differ from those of the original polymer. Free radicals can also be formed, and these may initiate and propagate chain degradation.<sup>8</sup> The predominating reaction depends on the polymer structure, radiation dosage, and temperature. Degradation may cause random chain scission or complete decomposition into monomer units.<sup>12</sup>

In this study, we used artificial aging processes to change the material properties of photopolymer printing plates in a systematic and controlled way. We studied the effects on the thermal properties of the photopolymer by means of differential scanning calorimetry (DSC). DSC is a useful technique for monitoring the effects of the aging or degradation of polymers.<sup>13,14</sup> Polymer degradation or crosslinking can cause changes in the thermal properties, such as shift in the polymer glass-transition temperature ( $T_g$ ) due to structural rearrangement or decreased flexibility.<sup>13</sup> Through the measurement of the  $T_g$  values

of UV-treated photopolymers, it is possible to record changes in polymer flexibility caused by aging effects. In addition, the changes in surface and cross-directional structures have been studied by microscopic analysis.

Studying the aging process gives useful information on the expected lifetime of photopolymers that can be used to predict detrimental effects on print quality. This refers to both the storage time (normal aging) and factors affecting the properties as a result of use (e.g., printing, washing, exposure to UV radiation, and heat in the print shop). In a parallel study<sup>15</sup> presented in a separate publication, we investigated the effect of simulated aging of plates on the print quality of coated paperboard.

## EXPERIMENTAL

### Materials

A digital printing plate (Nyloflex FAH-DII, Flint Group Printing Plates, Stuttgart, Germany) was used. Nyloflex FAH-DII is a monolayer plate with a Shore A hardness of 69° and is built up of a photosensitive polymer layer bonded to a polyester film for dimensional stability. The total thickness is 1.70 mm, of which the supporting polyester layer makes up 0.25 mm. The photosensitive layer consists of a styrene-diene elastomer, polymerizable low-molecular-weight acrylates and methacrylates, plasticizers, photoinitiators, stabilizers, and dyestuffs (Nyloflex safety datasheet). The elastomer consists of SIS rubber.<sup>16</sup>

### UV-induced aging of printing plates

All the printing plates were exposed to the normal prepress process described in Table I. Irradiation of the plate with ultraviolet radiation type A (UVA) with a wavelength of 365 nm during the main exposure step caused the photoinitiator molecules to absorb light and produce radicals, which then

TABLE II  
Simulated Aging Processes for the Printing Plates

Treatment	UV radiation		Exposure time	Radiative energy (MJ/m <sup>2</sup> )		
	Type	$\gamma$ (nm)		UVA	UVC	Total
Extended exposure in prepress						
2x UVA, 1 × main exposure	UVA	365	10 min	1.87	0.49	2.36
3x UVC, 2 × light finishing	UVC	254	2 × 8 min 45 s	1.14	1.48	2.62
4x UVC, 3 × light finishing	UVC	254	3 × 8 min 45 s	1.14	1.97	3.11
Exposure in QUV						
2h 340, UVA exposure at 60°C	UVA	340	1 + 1 h	2.86	0.49	3.36
4h 340, UVA exposure at 60°C	UVA	340	2 + 2 h	4.59	0.49	5.08
1cy 340, UVA exposure at 60°C	UVA	340	6 + 2 h	8.05	0.49	8.54
2cy 340, UVA exposure at 60°C	UVA	340	6 + 8 + 2 h	14.96	0.49	15.45

The radiative energy data refer to the total exposure, including the prepress process.

reacted with the monomer molecules. Propagation of this reaction process created a crosslinked network that altered the physical properties of the plate.<sup>2</sup> Crosslinked regions became solvent-insoluble in the washout process. After drying, postexposure to UVA radiation strengthened the plate and ensured thorough polymerization of extremely fine lines. Final ultraviolet radiation type C (UVC) irradiation at 254 nm was carried out to eliminate the tackiness of the printing plate.

The test images included areas of 20, 50, 70, and 100% tone value with a screen ruling of 34 L/cm. The size of the printing plates was 300 × 40 mm<sup>2</sup>. The print layout was created with a 20-W fiber laser with a resolution of 2540 dpi (CDI Classic Esko-Graphics, Gent, Belgium). The printing plates were exposed on the reverse side to UVA radiation in an exposure unit (BASF SACK LCX3, Kelva, Malmö, Sweden) to determine the relief depth and then were exposed on the print side to create the print layout. UVA radiation of 365 nm with an output energy of 1220 W/m<sup>2</sup> was applied in both cases. The printing plate was then washed for 20 min (Nylosolv II washing solution, Kelva) with a brushing pressure (i.e., nip distance) of 0.6 mm at a speed of 100 mm/min to remove the black laser layer and unexposed parts. After being dried, the plates were kept for a minimum of 6 h at room temperature to ensure complete evaporation of the washing solution. The plates were then postexposed to UVA (365 nm, 950 W/m<sup>2</sup>) and then finished (UVC, 254 nm, 940 W/m<sup>2</sup>) in an exposure unit (BASF Nyloflex FIV, Kelva).

The radiation classification, corresponding to the given wavelength, time of exposure, and radiation energy transferred to the printing plate in each step, is listed in Table I. The radiation energy was calculated by multiplication of the output energy of the lamps (W/m<sup>2</sup>) by the exposure time in seconds. The total exposure of UVA and UVC energy in the prepress process was thus 1.63 MJ/m<sup>2</sup>. The output

energy from the UV lamps decreased with time as an effect of age.<sup>2</sup> The main exposure unit was therefore equipped with a calibrated UV meter, and all the printing plates used in this study were exposed to the same quantity of radiative energy in the prepress process.

Some of the finished plates were exposed for extended times in the prepress process, as indicated in Table II. The rest of the plates were exposed to a simulated aging process with a QUV accelerated weathering tester (Q-Panel Lab Products, Bolton, United Kingdom) at Polystatic AB (Ängelholm, Sweden). Tests were carried out in accordance with ASTM G 154 with direct radiation without window glass. The process involved exposure to UVA radiation at 340 nm (240 W/m<sup>2</sup>) for a given time followed by 4 h of condensation (exposure to a saturated moist atmosphere) at 50°C, after which the plate was again exposed to UVA radiation for the specified time (e.g., 1 + 1 h in all). A full cycle according to the standard involved a total exposure of 8 h (the sample designated 1cy 340). One plate was exposed for two such UVA and condensation cycles (2cy 340).

The finished printing plates were stored horizontally and separately with a cellular plastic material facing the relief in a conditioned room (23°C and 50% relative humidity) away from sources of electrical charge, and they were protected from direct light by means of a black polyethylene plastic bag according to recommended storage conditions for an extended lifetime.<sup>11</sup>

DSC (DSC 2920 CE, TA Instruments, New Castle, DE) was used to study the effect of UV exposure on the thermal properties of the photopolymer plates. Samples from the top surface of the exposed photopolymer plates were collected from regions of solid-tone area by the careful slicing of a thin layer with a scalpel. The thickness of the sampling layer was 100–200  $\mu$ m as measured by a digital slide caliper, and this implied that the sample was taken from the

TABLE III  
 $T_g$ ,  $T_m$ , and  $\Delta H_m$  Values in the Surface Layer of Photopolymer Printing Plates

Printing plate	$T_{g1}$ (°C)	$T_{g2}$ (°C)	$T_m$ (°C)	$\Delta H_m$ (J/g)
Unexposed	$-64.7 \pm 0.2$	$37.0 \pm 1.0$	$-12.8 \pm 3.4$	$0.76 \pm 0.07$
Normally exposed	$-59.2 \pm 0.2$	$43.4 \pm 1.6$	$-11.8 \pm 1.2$	$0.66 \pm 0.44$
2x UVA	$-58.9 \pm 0.2$	$49.3 \pm 1.6$	$-13.6 \pm 3.3$	$0.65 \pm 0.02$
3x UVC	$-59.2 \pm 0.2$	$43.6 \pm 0.4$	$-11.9 \pm 0.6$	$0.64 \pm 0.15$
4x UVC	$-60.4 \pm 0.2$	$47.1 \pm 0.6$	$-7.8 \pm 3.1$	$0.70 \pm 0.12$
2h 340	$-55.0 \pm 0.2$	$49.4 \pm 0.6$	$-11.9 \pm 0.5$	$0.59 \pm 0.02$
4h 340	$-54.2 \pm 0.9$	$58.2 \pm 1.1$	$-10.3 \pm 1.4$	$0.62 \pm 0.05$
1cy 340	$-51.7 \pm 0.5$	$58.5 \pm 0.1$	$-13.8 \pm 1.1$	$0.56 \pm 0.22$
2cy 340	$-48.3 \pm 0.3$	$60.4 \pm 0.4$	$-13.2 \pm 0.6$	$0.63 \pm 0.09$

Averages and standard deviations from two measurements are shown.

upper tenth of the photopolymer height. Hermetically sealed, high-volume aluminum DSC pans were used, and the sample weight was  $12.0 \pm 0.6$  mg.

Temperature scans from  $-150$  to  $+200^\circ\text{C}$  were run to identify the temperature region of the glass transition(s) in the material;  $200^\circ\text{C}$  was set as the maximum because thermal decomposition began above this temperature (Nyloflex safety datasheet). Running at different scan speeds, including operation of the DSC instrument in the modulated mode, gave no indications of overlapping thermal transitions in the specified temperature range. All DSC measurements were therefore run in the standard mode from  $-135$  to  $+120^\circ\text{C}$  at a constant heating rate of  $10^\circ\text{C}/\text{min}$ .

The structural appearance of the UV-treated photopolymers was investigated with a Leo 1530 high-resolution field emission scanning electron microscope (Leo Electron Microscopy, Ltd., Cambridge, England). Samples about  $3\text{ mm} \times 10\text{ mm}$  in size were cut from the photopolymer plates with a scalpel and were mounted onto aluminum stubs by means of double-sided carbon tape so that either the surface or the cross-sectional side was directed upward for microscopic imaging. The stubs were fitted into a metal sample holder and placed in a vacuum chamber. The acceleration voltage was set to  $1.00\text{ kV}$  with a working distance of  $5\text{ mm}$ . Images were recorded at different magnifications ( $500$ ,  $2500$ , and  $10,000\times$ ) at several locations on the surface and at one magnification ( $1500\times$ ) on cross sections of the photopolymer plates. The latter were imaged to investigate any depth structural changes caused by penetration of the UVA or UVC radiation.

The chemical composition of the outermost photopolymer surface was quantified by electron spectroscopy for chemical analysis (Kratos AXIS Ultra<sup>DL</sup> X-ray photoelectron spectrometer, Kratos Analytical, Manchester, United Kingdom) with a monochromatic Al X-ray source. Before the analysis, the plate subjected to normal exposure was washed for  $30\text{ s}$  under isopropyl alcohol, ethanol, and water to remove any surface contaminants. The plate design-

ated 2cy 340 was selected for an in-depth analysis of aging effects (the sample was washed during exposure in the QUV chamber). The relative surface composition was obtained by quantification of detailed spectra run for each identified element. High-resolution carbon spectra were analyzed with respect to chemical shifts originating from carbon-oxygen bonds, thus providing information about the state of oxidation.

## RESULTS AND DISCUSSION

Polystyrene and polyisoprene are immiscible; this means that blends of these polymers show two glass transitions on a DSC heat flow curve. Functionalization by, for example, sulfonation can, however, create ionic interactions between the polymers to form miscible blends.<sup>17</sup> A sharp glass transition was found in all the sample types below  $0^\circ\text{C}$  with a corresponding change in the heat capacity of about  $0.3\text{ J/g }^\circ\text{C}$ . The  $T_g$  values (obtained from the inflection point) are shown in Table III. A second, weaker transition was also observed in the  $35$ – $60^\circ\text{C}$  temperature range. Repeated scans showed that both these transitions were fully reversible, with no temperature shift during the second scan. This is characteristic of a true glass transition. The origin of the low glass-transition temperature ( $T_{g1}$ ) is assumed to be the diene-rich phase of the elastomer. In the unexposed reference sample, this transition occurred at about  $-65^\circ\text{C}$ , which is in the midrange of literature data given for pure polyisoprene ( $-73$  to  $-55^\circ\text{C}$ ).<sup>18</sup>

The second glass-transition temperature ( $T_{g2}$ ) was less distinct and occurred over a broader temperature range (ca.  $15^\circ\text{C}$ ) with a correspondingly small change in the heat capacity (ca.  $0.03\text{ J/g }^\circ\text{C}$ , i.e., about one tenth of that at the low-temperature transition). This high  $T_g$  was recorded at about  $37^\circ\text{C}$  in the unexposed reference sample and was considerably lower than the  $T_g$  of pure polystyrene, which has a literature value of  $100^\circ\text{C}$ .<sup>18</sup> Similar results on SIS rubbers have been reported in a review by Hale and Bair,<sup>17</sup> and these could be explained by

extensive mixing of diene segments in the styrene phase or by a copolymer composition having styrene segments of a low molecular weight. Photopolymer plates usually have a composition with the flexible diene dominating over the more rigid styrene.<sup>3</sup>  $T_{g2}$  can also be influenced by the low-molecular-weight acrylates and methacrylates also present. The presence of plasticizers and fillers may also affect the location of the  $T_g$ .<sup>6</sup>

After normal exposure of the photopolymer plate, both  $T_g$ 's were shifted about 6°C upward (Table III). This shift was assumed to be related to the restrictions in chain mobility caused by the crosslinked network formed by polymerization of the acrylate monomers during UV exposure. Typical DSC curves are shown in Figure 1.

Doubling the main exposure (UVA 365 nm  $2 \times 10$  min) did not cause any significant shift in  $T_{g1}$ , whereas  $T_{g2}$  was increased another 6°C. Nor did posttreatment with UVC (254 nm for 8 min 45 s) for two or three times change  $T_{g1}$ . In the latter case,  $T_{g2}$  was, however, increased by about 4°C (Table III). Exposure of the photopolymers to UVA radiation at 340 nm for 2 or 4 h caused  $T_{g1}$  to be shifted about 5°C upward. There was also a significant effect on  $T_{g2}$ , with a 6°C increase after 2 h of exposure and a 15°C increase after 4 h, in comparison with the normally exposed photopolymer. The largest effect on  $T_{g1}$  was, not unexpectedly, observed for the samples exposed for one or two cycles. In the latter case, an upward shift of 11°C was observed. Simultaneously,  $T_{g2}$  was raised by 17°C. The crosslinking density is believed to increase as a result of exposure to UV radiation. An increase in the crosslinking density should affect the viscoelastic properties of the polymer,<sup>6</sup> and this would explain the shift of  $T_g$  to a higher temperature with prolonged exposure time. The data indicate that not only the photopolymerizable parts were affected by UV curing; the simulated aging also had an impact on the thermal properties of the basic SIS polymer.

Another interesting feature of the DSC curves of the photopolymers exposed for one or two cycles was the appearance of a third, weak glass transition around 38°C (Fig. 1). Overexposure to UV radiation with subsequent polymer degradation can result in a decrease in the crosslinking density.<sup>6</sup> The occurrence of this third  $T_g$  located at a temperature close to  $T_{g2}$  of the unexposed polymer thus strongly indicated a breakup of the crosslinked network. All three glass transitions were, however, less distinct than those in the normally exposed sample curve.

Between the two  $T_g$ 's, an endothermic peak was identifiable (Fig. 1). The reversibility of this transition was confirmed by repeated scans, and this suggested that its origin was a melting of crystallites rather than a simple endothermic relaxation due to a

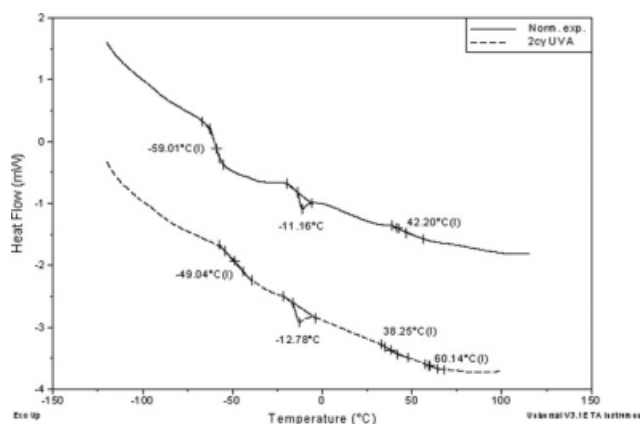


**Figure 1** DSC heat flow curves of the normally exposed photopolymer plate and the plate exposed for two cycles in the QUV tester. The curves show the thermal transitions (with exothermic heat flow in the upward direction) and have been vertically shifted for clarity.

release of a built-in strain in the polymer during aging.<sup>13</sup> However, the reproducibility of this transition was not as high as that of the  $T_g$  values because the value for the melting temperature ( $T_m$ ; the peak temperature, i.e., the temperature at the minimum of the endothermic peak) differed significantly between samples taken from the same photopolymer. Most of the curves showed, however, a  $T_m$  value in the range of  $-11$  to  $-13^\circ\text{C}$  with a change in the melting enthalpy ( $\Delta H_m$ ; given as the area under the curve from the initial transition temperature to the final transition temperature) of about 0.5–0.7 J/g.

Although the crystallization and melting of polyisoprene rubbers well below room temperature have been reported,<sup>14</sup> no such melting in pure SIS triblock copolymers is normally observable by DSC in the temperature range of  $-80$  to  $120^\circ\text{C}$ .<sup>17</sup> Because this transition was also present in the unexposed sample, its origin probably is either the acrylate or methacrylate monomeric components or the nonpolymeric additives. Literature values of  $T_m$  for isoprene and styrene monomers are  $-146$  and  $-30^\circ\text{C}$ , respectively.<sup>19</sup>  $T_m$  values below  $0^\circ\text{C}$  for a number of acrylate and methacrylate monomers have also been reported, whereas the  $T_m$  values for pure polyisoprene ( $26$ – $74^\circ\text{C}$ ), pure polystyrene ( $242^\circ\text{C}$ ), and a number of acrylates<sup>12</sup> are far above the observed region for this transition.

The observed variations in  $T_m$  can be explained by imperfect crystallization, melting under nonequilibrium conditions, or the presence of impurities (additives). Data for all samples are given in Table III. The observed increase in  $T_m$  for the 4x UVC sample may indicate a higher degree of crosslinking in line with the observed effects on  $T_{g2}$ . On the other hand, long-term exposure to UVA (one or two cycles) leads to a relocation of  $T_m$  close to the value

obtained for the unexposed sample ( $-13^{\circ}\text{C}$ ), suggesting a breakup of the crosslinked network and a return to monomer units.

The cold resistance, that is, the maintenance of mechanical properties at low temperatures, of diene rubbers is generally good. Subjecting the photopolymer to extremely low temperatures for a short time during the DSC scan is thus not likely to be detrimental. Isoprene rubber has, however, limited heat resistance and should not be kept at temperatures above  $70^{\circ}\text{C}$  for a long time. Styrene–isoprene copolymers are heat-resistant up to temperatures around  $120^{\circ}\text{C}$  and are more resistant to aging processes than the corresponding homopolymers are.<sup>20</sup> In the weathering tester, the plates were exposed to a temperature of  $60^{\circ}\text{C}$  during UV radiation, that is, well below this upper temperature limit. However, finished photopolymer plates should normally not be stored at temperatures above  $38^{\circ}\text{C}$ .<sup>11</sup> Oxidation is accelerated at high temperatures,<sup>8</sup> and the presence of weak points in the polymer chain and impurities can initiate polymer degradation at lower temperatures. The lack of endothermic transitions in the high-temperature range (confirmed by the initial DSC scans) indicates that the polymers did not undergo any thermal degradation during the short time intervals prevailing during the thermal analysis operations in this study. In other words, the observed changes in thermal behavior should be related solely to UV-induced effects.

Samples exposed in the QUV tester were also subjected to a hot condensing humidity for a period of 4 h or more. Exposure to hot moisture is commonly used to exaggerate aging effects of polymers (weathering testing). In the case of printing plates, exposure to hot water simulates the cleaning process after finalization of a print job. Absorption of liquid water or moisture can cause swelling or plasticization of many polymers. Polyolefins and rubber materials often show low water absorption,<sup>20</sup> and an increase in the crosslink density further reduces swelling.<sup>6</sup>

The swelling behavior of the normally exposed photopolymer plate was recorded via the weighing of small pieces before and after (1) storage in a climate chamber at  $50^{\circ}\text{C}$  and 98% relative humidity for 4 h (corresponding to the condensation step in the QUV chamber) and (2) soaking in water at  $23^{\circ}\text{C}$  for 24 h.<sup>3</sup> The ready-to-use normally exposed plate was chosen to record the effect of hot moisture solely, that is, with no uncontrollable side effects caused by exaggerated UV exposure. The results showed that any slight weight changes were within the error limits of the analytical balance (fourth decimal place); that is, there was no measurable water uptake under any of the testing conditions.

Furthermore, none of the samples exposed in the QUV tester showed a tendency to any reduction of

$T_g$ , which should otherwise be indicative of plasticization by water–polymer interaction. It is thus probable that the exaggerated UV radiation controlled the polymer properties and that the exposure to hot moisture, even under extreme conditions, had no significant effect. In the flexographic printing industry, photopolymers are normally demounted from the printing cylinder, placed vertically in a washing unit, and cleaned at a low temperature with a soft brush and a mixture of tap water and a cleaning liquid; this is followed by drying with a sponge roll. The whole procedure takes only 5–10 min. In contrast to this mild cleaning process, the plates are exposed to higher mechanical impact and also undergo significant swelling during the solvent washout step in the prepress process, including drying at  $60^{\circ}\text{C}$  for 1–3 h to completely deswell the plate.<sup>21</sup> Finally, the Nyloflex FAH-DII printing plate is recommended for alcohol- and water-based inks by the manufacturer and is thus resistant to such solvents after normal prepress processing.<sup>7</sup>

### Structural effects of UV-induced aging

Figure 2 shows scanning electron microscopy (SEM) micrographs (top view) of the various materials. The normally exposed photopolymer surface (top left) appears smooth with only a few visible features. After the main exposure to UVA for  $2 \times 10$  min (top right), a rougher surface with superficial streaks and cavities can be seen. Liu et al.<sup>1</sup> reported that no cracks were observable on a photopolymer plate of 1.14-mm thickness after exposure for up to 25 min. However, because they used a lower power during the main exposure step, the resulting UV energy received by the plate surface was only about half the energy to which the photopolymer designated 2x UVA was subjected in our study.

Postexposure to UVC twice, that is, a total of three radiation finishing steps (second row, left), resulted in a wrinkled surface similar to elephant skin. When samples were taken for DSC analysis from UVC-treated polymers, it was also observed that the topmost layer was easily separated from the bulk; that is, it could be lifted off as a “skin”. This was indicative of the formation of an oxidized layer that resulted in crazing of the surface, which could then be abraded off.<sup>9</sup> A total of four exposures to UVC radiation led to a very brittle surface. Severe damage to the polymer surface can be seen, with large, deep cracks (second row, right). Liu et al.<sup>1</sup> also reported the appearance of cracks when the exposure time in the radiation finishing process was extended from 8 to 20 min.

Two hours of UVA exposure led to severe cracking of the polymer surface (third row, left). The surface is divided into blocks, which seem to have

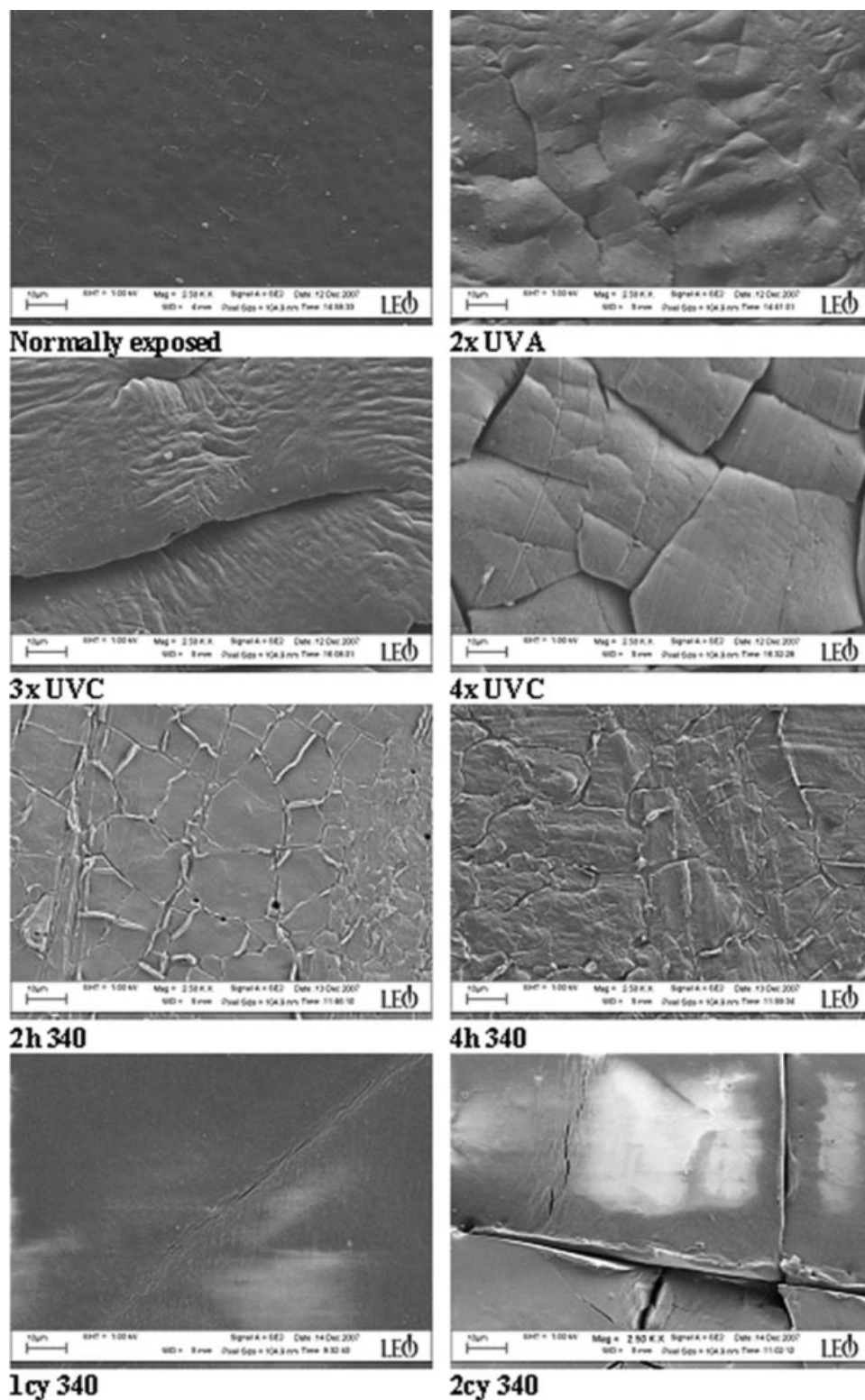
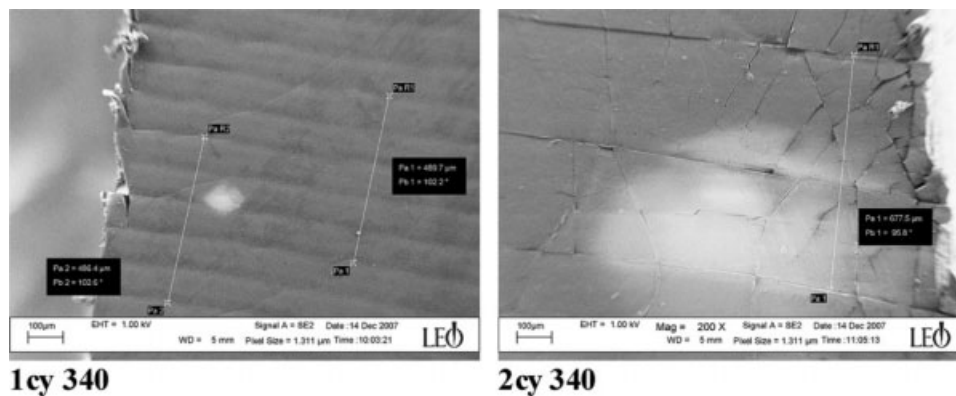


Figure 2 SEM micrographs of the photopolymers (top view; scale bar = 10 µm).

moved in relation to one another, almost like the effect of an earthquake. Deep holes penetrating into the structure can also be seen. Four hours of exposure to UVA led to a similar structure (third row, right). In addition, the topmost layer developed a wrinkled texture.

The top view of photopolymers exposed to one cycle of UVA radiation revealed the presence of very regular stripes or cracks on the surfaces. The bottom left image in Figure 2 shows one such crack. Software analysis shows that the distance between these cracks was 95–100 µm (Fig. 3). In the case of



**Figure 3** SEM micrographs of the photopolymers (top view) exposed for one or two cycles in the QUV tester. The micrographs show the regular occurrence of cracks (scale bar = 100  $\mu\text{m}$ ).

two cycles of UVA exposure (Fig. 2, bottom right image), these cracks were very deep with separated edges. These were in fact also visible to the naked eye and probably represent fatigue wear. The distance between the cracks was 300–330  $\mu\text{m}$  (Fig. 3). An analysis of the macroscopic surface roughness by means of a chromatic aberration sensor also revealed the presence of such regular stripes in the normally exposed plate in both full-tone and half-tone areas.<sup>15</sup> The parallel cracks were probably due to the fiber-laser ablation of the black laser layer when the print layout was formed on the plate. The fiber-laser beam was split into four separate beams to increase the ablation area and decrease the time for ablation. The distance of 95–100  $\mu\text{m}$  was probably the distance between the split beams, and the distance of 300–330  $\mu\text{m}$  was the total fiber-laser diameter, where two beams overlapped. It seems that these macroscopic laser beam artifacts also changed the photopolymer structure on a microscopic scale, and extensive cracking in their vicinity occurred after long-term exposure to UVA radiation. The regular stripes also influenced the print quality on solid-tone areas and on dots having a diameter exceeding approximately 220  $\mu\text{m}$ .<sup>15</sup> Two cycles of UVA exposure in the QUV tester also caused changes in the chemical and surface energetic properties.<sup>15</sup>

In addition to these parallel cracks, smaller cracks propagating in other directions could be seen, particularly near the edge. These smaller cracks probably arose during sample cutting for SEM analysis because the increased brittleness of the surface layer after extensive UVA exposure had made the polymer more sensitive to abrasive wear since no such easily damaging effects were observed in the samples exposed for shorter time periods.

Images of cross sections of the photopolymers were recorded sequentially from top to bottom to obtain images over the thickness of the photopolymer plates at a high resolution. Each image covered

a depth of about 150  $\mu\text{m}$ . Figure 4 shows the top-most of these sequential images for each photopolymer, with the surface directed toward the right.

The image of the normally exposed photopolymer plate shows a smooth cross-sectional surface. A weak stratal structure originating from the sheet-forming process can also be discerned. Also visible is the presence of some debris and small pits, probably originating from abrasion by the knife during sample cutting. UVA ( $2 \times 10$  min) did not greatly change the appearance of the photopolymer depth profile (top right image). Treatment with UVC (second row in Fig. 4) led to a very rough topmost layer that was clearly different from the rest of the structure. The depth of this layer was measured to about 20  $\mu\text{m}$  by the software. The increased number and depth of cavities present below this layer indicated enhanced brittleness of the photopolymer, that is, a greater risk that the material would be torn away upon cutting. The effect was more pronounced for the sample exposed 4 times. Two or four hours of exposure to UVA led to a very irregular cross-sectional surface (third row in Fig. 4), and it is evident that the UV radiation penetrated the photopolymer structure more deeply than in the case of normal or overexposed samples. The presence of such structural irregularities increased with increasing time in the weathering tester. A possible explanation could be shrinkage of the topmost surface layer.

Exposure to one or two cycles of UVA radiation led to a very rough topmost layer. A closer investigation of the deep cracks located near the edge in the sample exposed for two cycles showed that the cracks propagated as far as 35  $\mu\text{m}$  into the structure (Fig. 5). This is characteristic of fatigue wear.<sup>6</sup>

When all sequential images were collated into a single picture showing the full depth profile of the photopolymers, it was evident that the normal prepress process affected only a very thin surface layer of the plate structure (Fig. 6). The same was true for



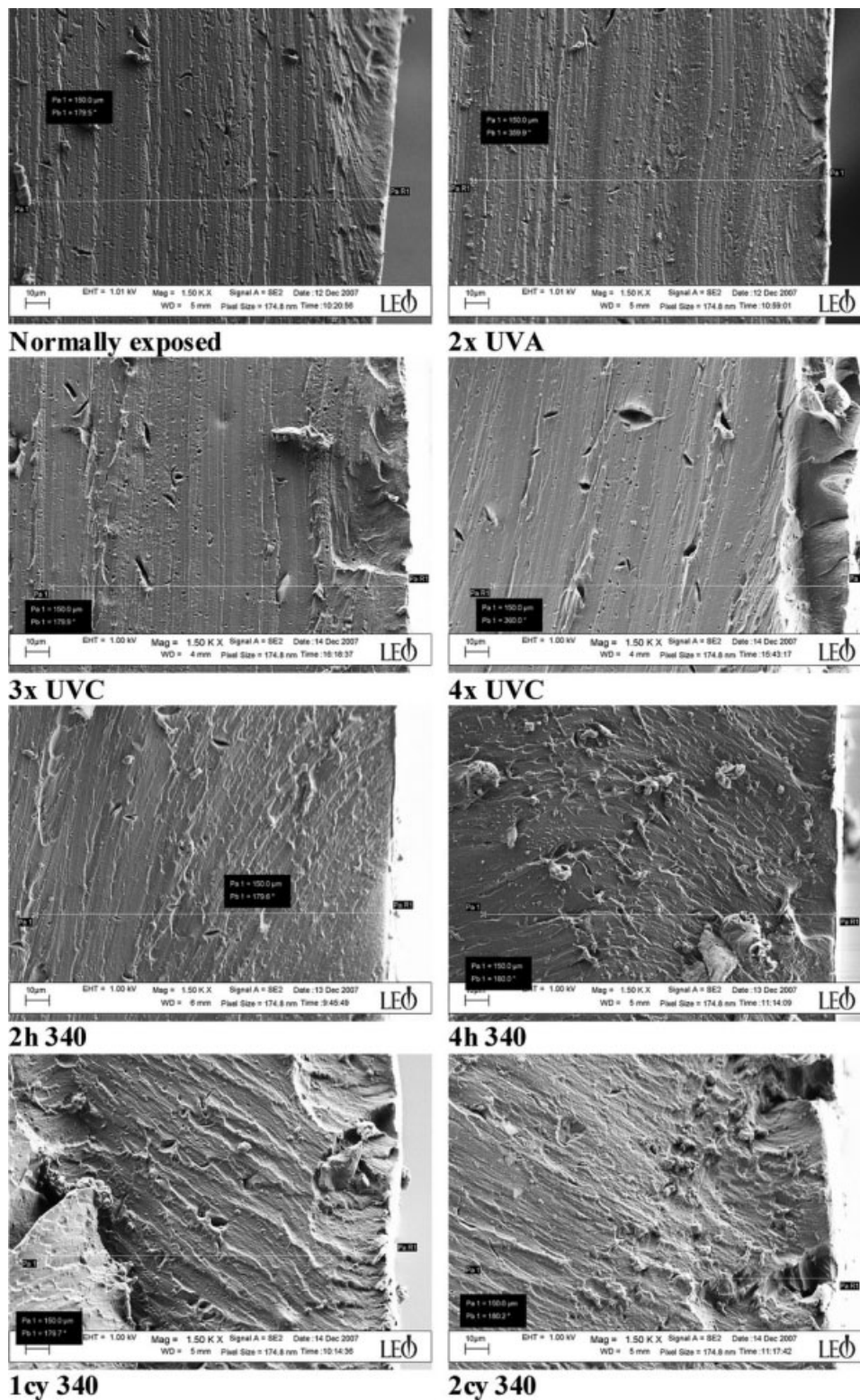
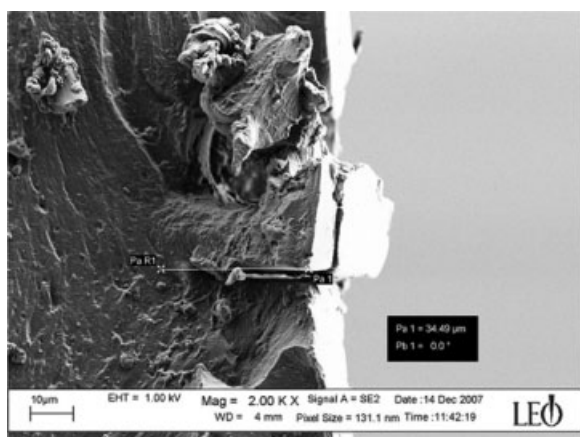


Figure 4 SEM micrographs of the photopolymers (side view; scale bar = 10 μm).

the plate exposed to UVC radiation four times in the light-finishing exposure unit (Fig. 6, middle row). Prolonged exposure to UVA radiation in the weathering tester resulted in a change in the structure at a deeper level, which was seen as a rougher texture

with a large number of cavities. Roughly estimated, one cycle of UVA exposure led to a change in the profile down to a depth of about 300 μm (not shown), whereas two cycles of UVA exposure affected the structure down to about 600 μm; this



2cy 340

**Figure 5** SEM micrograph of the photopolymer (side view) exposed for two cycles in the QUV tester. The micrographs show the depth of the edge-located cracks (scale bar = 10 μm).

was clearly seen as the deviant appearance of the top four sequential images at a depth of 150 μm each (Fig. 6). Below this level, the bulk photopolymer structure was similar to that of the normally exposed photopolymer.

### Surface chemical composition

The relative surface composition (atom %) and the chemical shifts in the carbon signal due to different functional groups are shown in Table IV. The main components are carbon and oxygen. The table clearly shows that the sample degraded in the QUV chamber contained more oxygen than the normally exposed sample, thus indicating that an oxidation process occurred; this also explains the observed decrease in polymer flexibility<sup>9</sup> seen as a shift in  $T_g$

(Fig. 1). The high concentration of C2 carbons also suggests that oxidation of the styrene-isoprene parts occurred because the relative amounts of C2 and C4 carbons were identical in acrylates and methacrylates. Also present in the uppermost surface was a small amount of nitrogen.

### Influence of the UV radiation wavelength

UVA and UVC radiation represent different energies because of their different wavelengths. The energy of a photon radiated at a given wavelength ( $E$ ) is commonly given by

$$E = \frac{hc}{\lambda}$$

where  $h$  is Planck's constant ( $6.63 \times 10^{-34}$  J s),  $c$  is the velocity of light in air ( $3.00 \times 10^{10}$  cm/s), and  $\lambda$  is the wavelength. Thus, 1 mol of photons of UVA radiation at 365 nm corresponds to an energy of 328 kJ/mol, whereas the same quantity of UVC radiation at 254 nm provides an energy of 471 kJ/mol. Expressed in electron volts, the energy that can be absorbed by the photopolymer by radiation with one photon of UV radiation is 3.4 (UVA) or 4.9 eV (UVC). Exposing the polymer plate to the same number of photons will thus cause a higher amount of energy to be transferred in the case of the more energy-rich UVC by a factor of 1.4. However, because the radiation wavelength of UVC is shorter than that of UVA, UVC should be less effective in penetrating the polymer plate.<sup>1</sup> It is thus expected that irradiation with UVC will lead to a higher cross-linking density in the surface layer already at short exposure times, whereas UVA radiation that penetrates more deeply is more likely to cause physical changes in the bulk material of the photopolymer plate, as was indeed observed in the sampling process and in the SEM analysis.

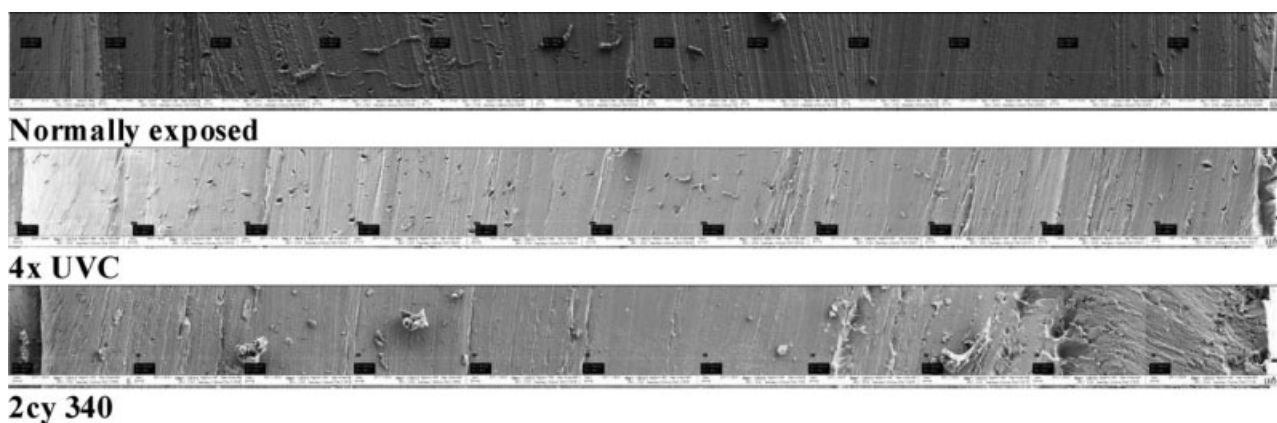


**Figure 6** Collated SEM micrographs of the cross-sectioned photopolymers. The micrographs show the changes in the structure as a function of the depth as an effect of UV irradiation. The top surface is directed toward the right.

**TABLE IV**  
**Relative Surface Compositions of the Elements**

Element	Release surface composition (atom %)	
	Normally exposed	2cy 340
C <sub>tot</sub>	96.0 ± 1.1	84.9 ± 1.1
C <sub>1</sub>	92.6 ± 1.2	65.2 ± 2.3
C <sub>2</sub>	2.6 ± 0.1	15.0 ± 0.1
C <sub>3</sub>	0.5 ± 0.1	3.2 ± 0.5
C <sub>4</sub>	0.5 ± 0.1	1.6 ± 0.3
O	4.0 ± 1.1	14.6 ± 0.9
N	—	0.3 ± 0.0
Si	<0.1	<0.1

The total amount of carbon (C<sub>tot</sub>) is divided into unoxidized carbon (C<sub>1</sub>), carbon with one bond to oxygen (C<sub>2</sub>), carbon with two bonds to oxygen (C<sub>3</sub>), and carbon with three bonds to oxygen (C<sub>4</sub>).

### CONCLUSIONS

This study has clearly shown that overexposure of flexographic printing plates can lead to dramatic changes in the polymer structure and properties. Long-term exposure to UVA radiation also causes severe polymer oxidation. The energy-rich, short-wave UVC radiation is more likely to damage the outermost surface layer, whereas UVA radiation has the ability to penetrate the structure more deeply and thereby affect the bulk polymer. Exposure to hot moisture did not seem to change the polymer properties.

Jens Ekengren is acknowledged for skilful operation of the SEM instrument.

### References

- Liu, X.; Guthrie, J. T.; Bryant, C. *Surf Coat Int B* 2002, 85, 243.
- Kannurpatti, A. R.; Taylor, B. K. *Flexo* 2001, 26, 12.
- Liu, X.; Guthrie, J. T. *Surf Coat Int B* 2003, 86, 91.
- Galton, D. *Flexo* 2007, 32, 44.
- Crouch, J. P. *Flexography Primer*, 2nd ed.; GATF: Sewickley, PA, 2003.
- Sutherland, J. E. *Technical Association of the Graphic Arts (TAGA) Conference Proceedings; TAGA: Rochester, NY, 1982; p 311.*
- Stemper, G. *Flexo* 1988, 13, 118.
- Harper, C. A.; Petrie, E. M. *Plastics Materials and Processes: A Concise Encyclopedia*; Wiley: Hoboken, NJ, 2003.
- Mark, J. E.; Erman, B.; Eirich, F. R. *The Science and Technology of Rubber*, 3rd ed.; Elsevier: Burlington, MA, 2005.
- Seckel, R. A. *Corrugating International*, August 2003. <http://www.tappi.org> (accessed October 2008).
- Blair, H. *Flexo* 2007, 32, 36.
- Stevens, M. P. *Polymer Chemistry: An Introduction*, 3rd ed.; Oxford University Press: New York, 1999.
- Hutchinson, J. M. *Prog Polym Sci* 1995, 20, 703.
- Sircar, A. K. In *Thermal Characterization of Polymeric Materials*, 2nd ed.; Turi, E. A., Ed.; Academic: San Diego, 1997; p 887.
- Johnson, J.; Andersson, C.; Lestelius, M.; Järnström, L.; Rättö, P.; Blohm, E. *Nordic Pulp Pap J*, submitted.
- Neumann, H. *Flint Group*, Stuttgart, Germany, personal communication, 2008.
- Hale, A.; Bair, H. E. In *Thermal Characterization of Polymeric Materials*, 2nd ed.; Turi, E. A., Ed.; Academic: San Diego, 1997; p 745.
- Peysen, P. In *Polymer Handbook*, 3rd ed.; Brandrup, J.; Immergut, E. H., Eds.; Wiley: New York, 1989; p VI/209.
- Fleischer, D. In *Polymer Handbook*, 3rd ed.; Brandrup, J.; Immergut, E. H., Eds.; Wiley: New York, 1989; p III/1.
- Alvear, C. *Plast & Gummilexikon*; Consulting European Association: Gothenburg, Sweden, 1997.
- Kannurpatti, A. R.; Taylor, B. K. *Flexo* 2002, 27, 31.